Exploiting Multi-Cell Battery for Mobile Devices: Design, Management, and Performance

Sungwoo Baek, Minyoung Go, Seokjun Lee and Hojung Cha
Yonsei University
Department of Computer Science
Seoul, Republic of Korea
{swbaek,mygo,sjlee}@mobed.yonsei.ac.kr,hjcha@yonsei.ac.kr

ABSTRACT

Extending battery lifetime is an important issue for mobile devices. While extensive attempts have been made at the software level, optimization often risks hampering user experience. One fundamental method to increase battery lifetime is to improve the efficiency of the battery itself. We argue that the multi-cell battery system, which is widely used for enhancing battery efficiency in the electric vehicle (EV) field, can solve this issue. However, due to the hardware constraints and device usage characteristics, battery advancements in the EV field are not directly applicable to mobile devices. In this paper, we propose BattMan, a multi-cell battery management system for mobile devices, for the enhancement of battery efficiency. We develop an accurate battery cell model to estimate the expected battery lifetime considering the recovery effect, the rate capacity effect, and battery aging. We also propose a multi-cell scheduling algorithm to maximize the overall battery lifetime. We implemented BattMan on recent smartphones and evaluated its impact on battery lifetime. The experimental results show that a two-cell configuration of the proposed system increases battery lifetime by an average of between 14-19%, depending on cell aging, in real usage scenarios over a single-cell battery of the same overall capacity. We hope the proposed multi-cell battery scheme opens up a new direction towards battery lifetime improvement in mobile devices.

CCS CONCEPTS

• **Computer systems organization** → **Embedded systems**; • **Hardware** → **Batteries**;

KEYWORDS

Mobile devices, Battery lifetime, Multi-cell battery, Battery management system, Cell modeling

1 INTRODUCTION

As the functionality of mobile applications grows more versatile and complex, the demand for high performance mobile devices rapidly increases. In the case of Central Processing Units (CPUs), the number of cores and the operating frequency have steadily increased, leading to high battery consumption. However, battery capacity has improved slowly relative to device performance. Figure 1 illustrates the trend of CPU performance and battery capacity for Samsung's Galaxy series of smartphones. The expansion of the battery capacity is significantly slower than that of the CPU. The battery capacity of the Galaxy S6 has even decreased due to design issues.

Extending device lifetime is a fundamental issue for mobile devices. Diverse approaches have attempted to prolong battery lifetime, such as software optimization [25], constraining hardware performance [33], and device idle time management [11]. Software-based methods often result in performance issues along with user experience tradeoffs. Since the degradation of user experience is unavoidable in most cases, the software-based approach should be carefully applied in real environments. Increasing device lifetime without any impairment of user experience is an ideal solution. To this end, one intuitive approach is to enhance battery performance itself.

There are several methods for improving batteries that result in enhanced device lifetime. First, battery capacity can be augmented by increasing the battery size or utilizing new materials in battery production. However, this is unlikely to happen in imminent future, because battery size tends to be smaller and thinner for design purposes, and developing new battery materials is challenging indeed. Another solution is to improve battery efficiency. For example, multi-cell batteries could be exploited even for mobile devices. In fact, a multi-cell battery system that consists of several

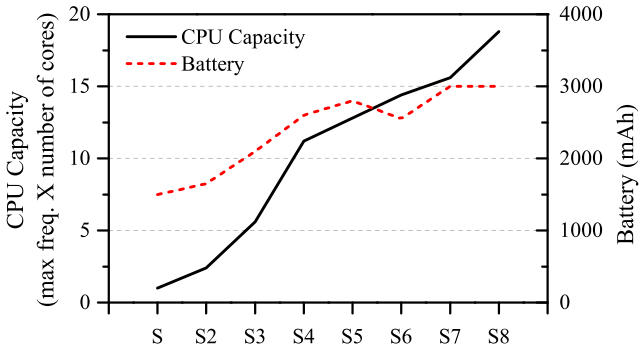

Figure 1: CPU performance vs. battery capacity for Samsung Galaxy series of smartphones (Sx represents the device model)

SenSys '17, November 6–8, 2017, Delft, Netherlands

ACM ISBN 978-1-4503-5459-2/17/11…$15.00
https://doi.org/10.1145/3131672.3131684

small battery cells instead of a single large one is commonly employed in the EV field. With a multi-cell system, battery lifetime can increase with the active use of battery characteristics, such as the rate capacity effect [15] or recovery effect [6]. The rate capacity effect means that the battery cell's voltage drops rapidly under a high discharging current, and the recovery effect means that the cell voltage recovers itself when discharged intermittently. Battery lifetime can therefore be extended with an adequate battery usage policy, which exploits the concurrent discharging of multiple cells, or intermittent discharging, by switching component cells appropriately. This opens up a new opportunity to increase battery lifetime even in mobile devices.

To maximize the lifetime of a multi-cell battery system, the use policy for each constituent cell should be accurately determined at runtime, because the recovery effect and rate capacity effect exhibit different characteristics depending on the discharging current and the number of cells employed in the system. Moreover, the use policy should reflect the degree of cell aging or degradation, often called the State of Health (SoH) of the cell, because the degraded battery cell significantly affects both the recovery effect and the rate capacity effect. This brings us a big challenge, i.e., battery cell modeling. In order for the multi-cell battery system to work in mobile devices, the battery itself should be modeled to predict the battery lifetime accurately considering the battery characteristics mentioned above. Since the characteristics are affected by various factors such as discharging current, length of consecutive discharging, frequency of cell switching, and degree of aging (i.e., SoH), the battery model should be developed precisely. Unfortunately, regarding the lifetime aspect of battery analysis, previous cell models are not accurate, specifically due to lack of consideration for the recovery effect and SoH. For example, the battery circuit model [17] does not address the SoH factor for the changes in cell capacity and internal resistance. Similarly, the electrochemical models [14, 31] and diffusion models [29, 30] do not reflect the lifetime gain potentially acquired with the recovery effect.

The second challenge lies in the development of cell discharge scheduling for multi-cell battery systems, which would increase overall lifetime by maximizing both the rate capacity and recovery effects. To this end, a sophisticated algorithm should be developed to optimize cell usage. Since the discharging current tends to change frequently in mobile device, the algorithm should determine the best cell use policy with minimum overhead. Most previous research tried to increase battery lifetime considering only the recovery effect [7, 34] or the rate capacity effect [5, 27] independently. Although a few approaches [21] studied both effects, they did not reflect the SoH factor. In addition, since these studies primarily targeted the EV field, they required specific hardware to collect and the target is limited to the case of constantly-discharged current, which are not applicable to mobile devices. Thus, in order to exploit multi-cell batteries for mobile devices, we have to devise a cell use policy considering dynamic discharging current and SoH to reflect both the recovery effect and the rate capacity effect, consequently maximizing battery lifetime.

In this paper, we propose BattMan, a prototype of a multi-cell battery system specifically designed for mobile devices, to address these issues. We first developed a battery cell model to estimate its lifetime accurately, considering various factors such as discharging current, SoH, the rate capacity effect, and the recovery effect. Based on the existing equivalent circuit battery model, the proposed model was extended by specifically considering the additional factors of recovery effect and SoH. We then developed a multi-cell scheduling scheme called the weighted SoC-based round robin (WSRR) to select the best use policy which maximizes the efficiency of the rate capacity effect and the recovery effect. This allows BattMan to maximize the overall battery lifetime in the multi-cell configuration. To the best of our knowledge, BattMan is the first multi-cell battery system implemented in real mobile devices. Our contributions are as follows:

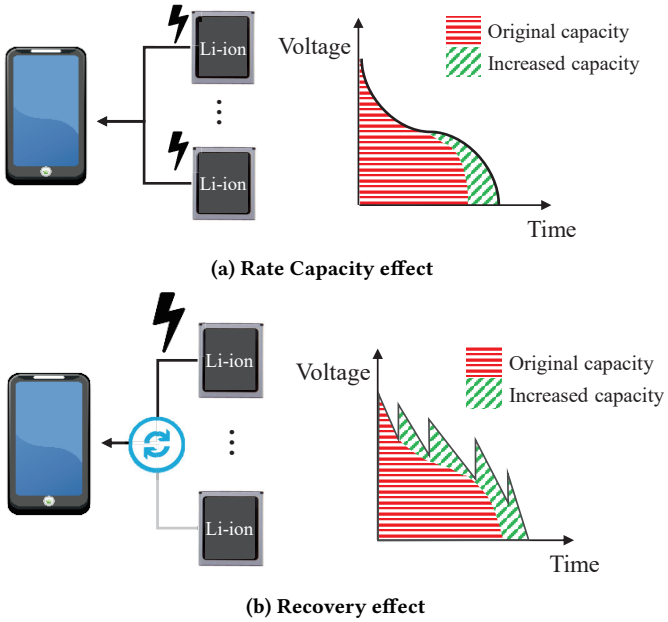

Figure 2: Potentials of multi-cell battery system

- We provide an accurate battery cell model to estimate the battery lifetime considering the rate capacity effect, the recovery effect, and the SoH factor. Also, a runtime algorithm for optimizing the multi-cell use policy is proposed to maximize battery lifetime.
- The proposed scheme is implemented in real mobile devices and delivers battery lifetime extension. Various experiments conducted in real application scenarios validate the effectiveness of the proposed scheme in terms of battery lifetime improvement.

2 MULTI-CELL BATTERY FOR MOBILE DEVICES

2.1 Multi-cell Battery System

A multi-cell battery system utilizes multiple cells instead of a single, large cell for its power source. As described above, two main phenomena of the battery—rate capacity effect and recovery effect—are exploited in the multi-cell configuration. Figure 2 shows the potentials of a multi-cell system over that of a single-cell battery. Figure 2(a) illustrates the concept of the rate capacity effect, that is, the available capacity of a battery cell changes subject to power

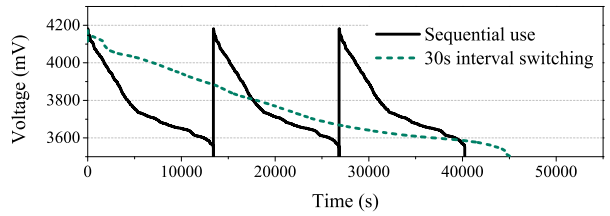

(a) Lifetime on recovery effect (three batteries).

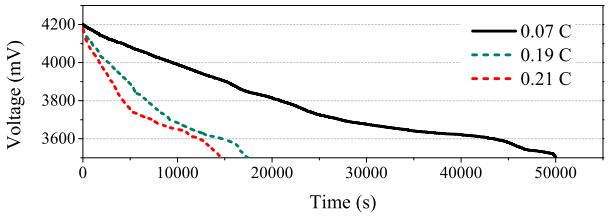

(b) Lifetime on rate capacity effect (a single battery).

Figure 3: Battery characteristics (Samsung Galaxy S4).

consumption: the smaller the power consumption, the larger the available capacity. Concurrent discharging of N cells would result in the power consumption of each cell reduced to $1/N$ and enlarge the available capacity. Figure 2(b) illustrates the effective use of the recovery effect. The voltage recovers itself when the cell becomes idle, hence battery lifetime could increase by switching multiple cells.

2.2 Preliminary Experiments

In order to observe the feasibility of exploiting recovery effect and rate capacity effect towards battery lifetime extension in real devices, we built a system to switch multiple batteries at runtime (refer Section 4 for the details). For the preliminary study, we used three brand-new standard batteries from the Samsung Galaxy S4 smartphone (2,600mAh capacity). While discharging the S4 smartphone with 0.21 C-rates[1] on average, we measured the voltage of the switching system and compared it with the case of sequential use of three batteries. Figure 3(a) shows that battery lifetime increased approximately 10% over sequential use when the three batteries were switched every 30 seconds. This is due to the recovery effect of each battery while resting in the idle state. Meanwhile, Figure 3(b) shows the voltage traces of a single battery exhibiting the capacity fade on different C-rates. The device runs about 833 min, or 97.2% of the theoretical capacity, at the average discharge rate of 0.07C, whereas the device runs 291 min (92.1%) at 0.19C and 243 min (85.3%) at 0.21C. The experiment shows that the rate capacity effect indeed exists in real device since there is additional capacity loss with a high discharge current.

Next, we compared the efficiency of the rate capacity effect and the recovery effect according to the battery aging (i.e., SoH). For the experiment, we solicited a number of Galaxy S4 batteries with varying degrees of SoH and repeated the experiment illustrated in Figure 3. Figure 4 shows the lifetime gain due to both the recovery effect and the rate capacity effect, according to SoH. Here, SoH is

[1]C-rate is defined as the discharge current divided by the theoretical current draw under which the battery cell would deliver its nominal rated capacity in one hour.

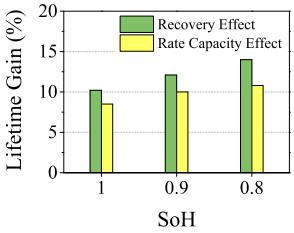

Figure 4: Lifetime vs. SoH.

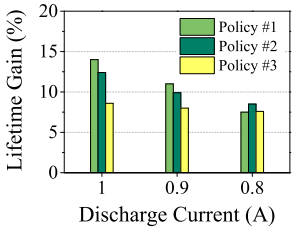

Figure 5: Effect of battery cell use policy.

calculated as the ratio of available capacity over design capacity. For example, SoH 1 in the figure stands for a brand-new battery. For the rate capacity effect, lifetime gain is calculated by comparing the case of 0.21C to that of 0.07C. The results in Figure 4 show that the efficiency of both effects increases with the degree of aging (i.e., toward low SoH).

We also demonstrate the necessity of an efficient cell use policy in multi-cell battery system. We used a three-cell battery for the experiment[2], where three different use policies are exercised: Policy #1 of concurrent discharging of all three cells (i.e., no cell switching), Policy #2 of discharging two cells, sequentially selected from three, and Policy #3 of discharging one cell at any time while recovering the remaining two. For Policy #2 and Policy #3, the cells are selected every three seconds in a round-robin fashion. Figure 5 shows that the best use policy which shows the maximum lifetime gain changes with discharging current. With low discharging current, utilizing recovery effect is more efficient while rate capacity effect is dominant under high discharging current. Since the rate capacity effect and the recovery effect are affected by many factors, the best policy changes accordingly.

Given these observations, we concluded that the multi-cell battery system shows actual lifetime gain, and determining the best battery usage policy is necessary to maximize battery lifetime.

3 BATTMAN DESIGN

3.1 System Overview

The goal of BattMan is to extend battery lifetime with the use of multi-cell configuration by exploiting potential electric energy. BattMan makes use of the recovery effect by resting the cells and also maximizes battery lifetime by splitting loads into multiple cells in a battery to reduce capacity fade. The BattMan system adaptively determines the cell use policy to maximize the battery lifetime using both effects. To this end, we developed a battery cell model that traces voltage to predict the expected battery lifetime considering the rate capacity effect, the recovery effect, and even SoH. Based on the proposed model, we designed a cell scheduling algorithm to maximize lifetime. Figure 6 shows the overall architecture of BattMan. The BattMan hardware monitors the device's discharge current, and also the status of each cell such as voltage, SoC, and SoH. Given the device workload, the discharging cells are appropriately selected and subsequently operated according to the best

[2]For this experiment, we simply used three 2,600mAh batteries for Galaxy 4. Therefore, a cell here represents a smartphone battery.

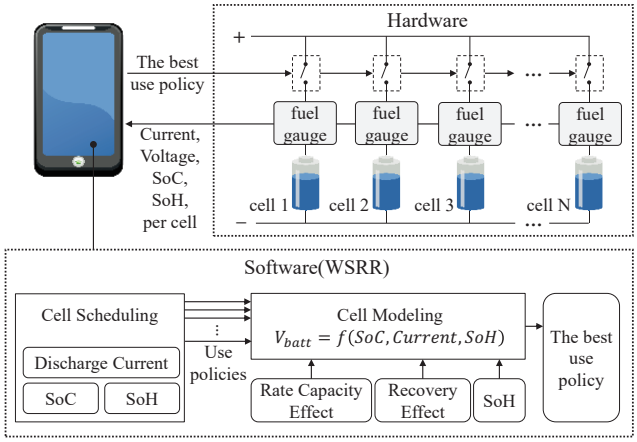

Figure 6: BattMan Overview.

use policy determined by the BattMan software, that is the WSRR scheme.

In the following section, we describe the equivalent circuit battery cell model that is the basis of our model. Our model is then extended to consider both the SoH and the lifetime gain due to the recovery effect. Finally, we detail the cell scheduling algorithm, which finds the best cell use policy given the discharging current.

3.2 Battery Cell Modeling

Existing Circuit Model. The electrical equivalent circuit model [23] is commonly used to predict a battery's voltage by modeling the battery as the combination of resistance and capacitance. Among the various models, the run time base two RC model [10] is the widely-used circuit model, consisting of series resistance, transient resistances, transient capacitances, and power source. Figure 7(a) illustrates an example of the second order RC model.

As illustrated in Figure 7(a), the circuit model is generally composed of two resistance-capacitance networks (RC networks). Figure 7(b) shows the battery cell's voltage trace according to discharging and recovering. Voltage change is divided into two factors: the instant voltage drop V_{drop} when discharging occurs, and the voltage drop upon discharging time $V_{transient}$. V_{drop} is modeled by R_s, whereas $V_{transient}$ is modeled by R_1, R_2, C_1, and C_2. The cell voltage V_{batt} is then calculated by subtracting the RC network's voltage from the open circuit voltage V_{OCV} as follows:

$$\begin{aligned} V_{batt} &= V_{OCV} - V_{transient} - V_{drop} \\ &= V_{OCV} - (V_1 + V_2) - I_d \cdot R_s \\ &= V_{OCV} - (I_1 \cdot R_1 + I_2 \cdot R_2) - I_d \cdot R_s \end{aligned} \tag{1}$$

where I_d is the actual discharging current, and I_1 and I_2 are the current of each RC network. To acquire V_{batt}, we have to model (a) OCV (open circuit voltage), (b) R_s, and (c) R_1, R_2, C_1, C_2.

First, OCV is modeled according to the state of charge (SoC). Since the cell voltage reaches OCV after recovering for more than one hour, OCV is modeled by resting the cell for each SoC. Series resistance R_s is calculated as:

$$R_s = \frac{V_{drop}}{I_d} \tag{2}$$

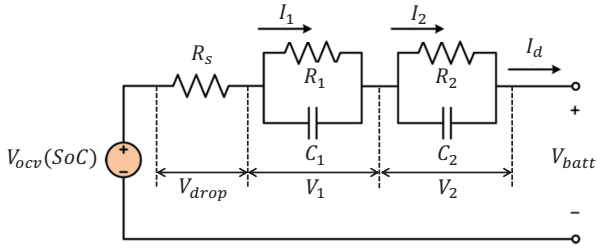

(a) Two RC network circuit model [10]

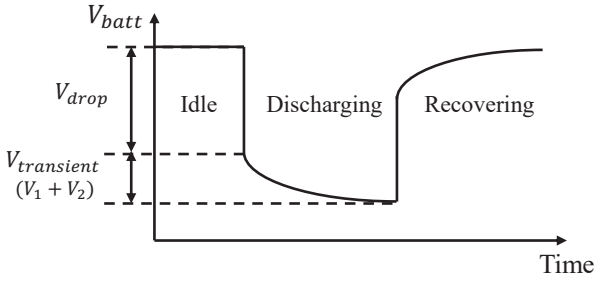

(b) Voltage curve.

Figure 7: The existing equivalent circuit model and the voltage curve of battery.

Here, V_{drop} is measured by the instantaneous voltage rise when cell starts to rest. Next, the capacitors and resistances of each RC network are modeled by observing $V_{transient}$. When the cell recovers after discharging more than 30 minutes, its voltage increases exponentially and finally reaches OCV. By fitting the voltage to time in exponential shape, R_1, R_2, C_1, and C_2 are calculated as:

$$\begin{aligned} V_{transient}(t) &= I_1(t) \cdot R_1 + I_2(t) \cdot R_2 \\ &= a \cdot \exp(b \cdot t) + c \cdot \exp(d \cdot t) \end{aligned} \tag{3}$$

$$R_1 = \frac{a}{I_1}, \quad R_2 = \frac{c}{I_2}, \quad C_1 = \frac{1}{R_1 \cdot b}, \quad C_2 = \frac{1}{R_2 \cdot d} \tag{4}$$

I_1 and I_2 are affected by C_1, C_2, and I_d. They can be calculated according to [20, 22]. Since V_{drop} and $V_{transient}$ depend on SoC, the parameters of circuit model also vary with SoC. Therefore, $X = \{R_s, R_1, R_2, C_1, C_2\}$ is fitted to SoC as an exponential shape:

$$X_i(SoC) = (e_i \cdot \exp(f_i \cdot SoC) + g_i) \tag{5}$$

The cell voltage V_{batt} is finally calculated as:

$$\begin{aligned} V_{batt}(SoC, I_d) = V_{OCV}(SoC) \\ - I_1(SoC, I_d) \cdot R_1(SoC) \\ - I_2(SoC, I_d) \cdot R_2(SoC) \\ - I_d \cdot R_s(SoC) \end{aligned} \tag{6}$$

Note that the accuracy of existing circuit model has been validated in various previous works [16, 35]. However, most of the existing models rarely consider cell aging or the lifetime gain due to recovery effect, because they only considered the SoC and discharging current.

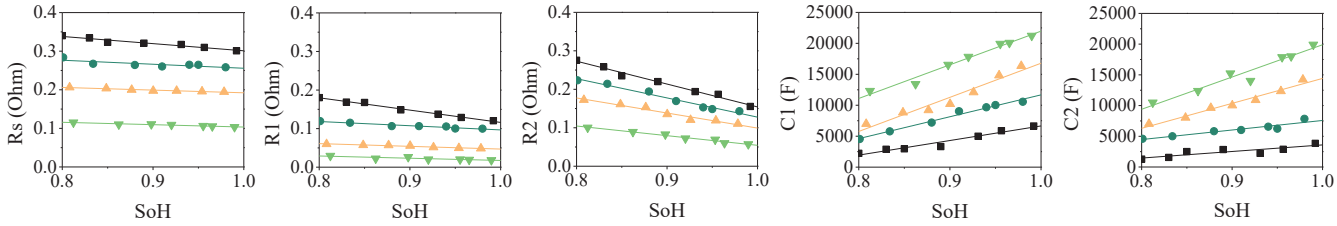

Figure 8: Experimental observations for SoH and various components of circuit model. Four different capacities of battery are tested; 450mAh (■), 600mAh (●), 900mAh (▲), 1800mAh (▼) with 50% of SoC. The trend lines are acquired with simple linear regression.

Reflecting SoH and Recovery Effect. We extend the existing circuit model to reflect battery aging and lifetime gain of recovery effect. As the number of charging/discharging cycle increases, a battery's internal resistance becomes larger. Since voltage is affected by resistance, both V_{drop} and $V_{transient}$ change with internal resistance. To model the SoH factor, we empirically observed the relationship between SoH and other components of the circuit model (see Section 5 for the experiment details). Figure 8 shows that SoH exhibits almost a linear relationship with R_s, R_1, R_2, C_1, and C_2. Based on our experimental observations, we modified $X = \{R_s, R_1, R_2, C_1, C_2\}$ to consider the degree of battery aging as:

$$X_i(SoC, SoH) = (e_i' \cdot \exp(f_i' \cdot SoC) + g_i') \cdot (h_i \cdot SoH + j_i) \quad (7)$$

Here, SoH indicates the ratio of available capacity compared to design capacity. The design capacity is pre-defined in mobile system, hence readily available. The available capacity can be acquired by using the fuel gauge in a mobile device, based on the Coulomb counting technique which calculates the capacity by accumulating the amount of discharged current.

Meanwhile, modeling the lifetime gain due to the recovery effect is difficult because the increased voltage during rest and the actual recovered capacity are not directly related. The existing circuit model cannot consider lifetime gain because the model only predicts the voltage, not a capacity. After analyzing the recovery effect and the circuit model in various aspects, we observed that the increased voltage during recovery is caused by the capacitances in RC networks. In other words, we consider that the electric charge is stored in capacitance during discharging and it is returned to battery in recovery phase, increasing cells voltage. Based on the key principle of circuit model which represents the recovered voltage as capacitance and also on our observations, we assume that some of the returned electric charge becomes the actual gain of capacity. Now, we model the capacity gain due to recovery effect $C_{recovered}$ as:

$$C_{recovered} = \rho \cdot (\int (I_1(t) + I_2(t))dt), \text{ where } I_d = 0 \quad (8)$$

where ρ represents the recovery coefficient. Thus, $C_{recovered}$ is calculated by multiplying ρ with the discharged capacity during rest. Note that the cell's remaining capacity is increased by $C_{recovered}$. This way, we reflect $C_{recovered}$ to the circuit model in terms of OCV. The final expression for V_{batt} is:

$$\begin{aligned} V_{batt}(SoC', I_d, SoH) = {} & V_{OCV}(SoC') \\ & - I_1(SoC', I_d, SoH) \cdot R_1(SoC', SoH) \\ & - I_2(SoC', I_d, SoH) \cdot R_2(SoC', SoH) \\ & - I_d \cdot R_s(SoC', SoH) \end{aligned}$$

$$SoC' = \frac{C_{used} - C_{recovered}}{C_{designed}} \quad (9)$$

where C_{used} is the amount of used capacity and $C_{designed}$ is the designed capacity of cell.

3.3 Parameter Extraction

The parameter extraction process for the proposed battery cell model includes observing the voltage trace according to SoC, discharging current, and SoH, as well as analyzing the capacity gain due to recovery effect. In this section, we describe the detailed methodology for parameter extraction.

First, we generate the OCV-to-SoC table. The battery cell is discharged by the battery cycler[3] and whenever SoC is changed by 1%, OCV is measured by resting the cell more than one hour. Since the minimum unit of SoC in our table is 1%, the fine-grained OCV is interpolated between SoCs. For example, V_{OCV} (50.7%) is calculated as $V_{OCV}(51\%) - (V_{OCV}(51\%) - V_{OCV}(50\%)) \cdot (51 - 50.7)$.

Next, we analyze the voltage trace under various SoC, discharging current, and SoH, to extract the parameters of our model. Since conducting experiments for all the possible combinations of parameters is not feasible, we selected a sufficient number of cases and extracted the parameters through data fitting. To acquire the level of SoH that we need, the cell is repeatedly discharged and charged with the cycler.

In order to calculate the recovery coefficient ρ, the actual capacity gain $C_{recovered}$ should be estimated. We acquire this by comparing the amount of used capacity when a cell is discharged intermittently with when a cell is discharged continuously. For example, when the cell is using 85% capacity for continuous discharging while 92% is being used for intermittent discharging, $C_{recovered}$ is 7% of capacity. The parameter values and the modeling results are described in Section 5.

[3]We used the Maccor series 4300K, shown in Figure 10, which is able to discharge and charge with ±5V and ±5A.

3.4 Cell Scheduling

Thus far, we have discussed the battery cell characteristics to maximize usage time. Concerning both recovery and rate capacity effects, BattMan selects the most efficient set of active cells, or the cells to use with the WSRR algorithm. We compare the lifetime of various use policies through our cell model and select the best use policy to maximize the battery lifetime. To this end, three problems should be resolved: how to generate the use policy, how to find the best use policy, and when to perform the cell switching algorithm.

Determining use sequence. We describe the determination of the use sequence which maximizes lifetime under a given number of discharging cells. The use sequence indicates the order of cell discharging, taking the form of double array. For example, when four cells are discharged sequentially, the use sequence is [[1,0,0,0], [0,1,0,0], [0,0,1,0], [0,0,0,1]]. On the other hand, when three out of four cells are discharged at a time, one of the possible use sequence is [[1,1,1,0], [0,1,1,1], [1,1,0,1], [1,0,1,1]], indicating the recovery order is #4, #1, #3, and #2. To maximize the lifetime, two conditions should be satisfied. First, we should balance the SoC of all cells as evenly as possible. When a cell is fully discharged much earlier than others, recovery opportunity will be reduced and discharging current for the rest of cells will become higher. This will decrease overall lifetime of the battery system. In addition, parallel connection of cells with different SoC would lead to inefficient discharging. Second, we should prevent the consecutive discharging of a particular cell as much as possible. Since the lifetime increases with recovery frequency, the discharging time should be minimized, leading a cell to rest as frequently as possible.

To fulfill the requirement above, we designed a scheme to determine use sequence. The scheme generates the use sequence which balances all cells' SoC and maximizes recovery frequency. The detailed algorithm is shown in the *SeqGen* function of Algorithm 1. Q means the amount of discharging capacity during each switching interval T. The SoC of each cell represents the remaining capacity as well as priority. W is a penalty constant for consecutive discharging. For every switching interval T, we determine the set of cells to use, that is, S. First, the *weighted_SoC* of each cell is calculated based on its SoC and the penalty $W^{C[i].usage}$ determined by the number of consecutive use (line 8-9). Next, the scheme selects N_d cells in order of *weighted_SoC* (line 11), and discharges the amount of Q for the selected N_d cells (line 12-20). Finally, S is added to use sequence *Seq* (line 20). The overall process is repeated until SoC of all cells becomes zero (line 21-23). Note that SoC of all cells becomes zero approximately at the same time because the SoC is directly related to the priority, leading SoC for all cells to be balanced naturally.

Finding the best use policy. The battery lifetime is affected by discharging current and recovery frequency. Therefore, minimizing the discharging current and maximizing recovery frequency for individual cells is important. These two factors are determined by the number of discharging cells. With a larger number of discharging cells, the current for individual cells decrease, so does the recovery opportunity. Thus, the number of discharging cells should be selected appropriately according to the required current load. The use sequence described earlier is unique for the number of discharging cells. For each number of discharging cells, BattMan generates the use sequence and estimates its expected lifetime. Among the use sequences, the one which maximizes lifetime is chosen.

Algorithm 1. Selecting discharging cells (WSRR).

Input: Number of cells N,
Cells C=$[C_1, \cdots, C_N]$,
Discharging current I,
Cut-off voltage V_{cutoff},
Switching interval T
Output: The cell usage policy

```
1.  func SeqGen(N, N_d, C, I)
2.    W ← Penalty constant for consecutive discharging
3.    Quantum Q ← I × T // the discharged capacity at once
4.    cell_to_use ← [], weighted_SoC ← []
5.    while true do
6.      S ← [] // the set of cells to use
7.      weighted_SoC ← [],
8.      for i ← 1 to N
9.        weighted_SoC[i] ← C[i].SoC × W^C[i].usage
10.     // find the N_d cells in the order of weighted_SoC
11.     cell_to_use ← FindMaxIndex(N_d, weighted_SoC)
12.     for i ← 1 to N
13.       if cell_to_use contains i do
14.         S[i] ← 1
15.         C[i].SoC ← C[i].SoC − Q
16.         C[i].usage ← C[i].usage + 1
17.       else
18.         S[i] ← 0
19.         C[i].usage ← 0
20.     Seq.append(S)
21.     for i ← 1 to N
22.       if C[i].SoC is 0
23.         break
24.   return Seq
25.
26. lifetime ← [], Seq ← []
27. for i ← 1 to N do
28.   lifetime[i] ← 0
29.   C.initialize() // reset the information about cells
30.   Seq[i] ← SeqGen(N, i, C, I)
31.   while true
32.     for S in Seq[i]
33.       lifetime[i] ← lifetime[i] + T
34.       for k ← 1 to N
35.         C[k].voltage = CellModel(C[k], S, I / i)
36.         if C[k].voltage < V_cutoff
37.           go to 27
38. N_best ← argmax_index(lifetime)
39. return Seq[N_best]
```

The detailed process is explained in Algorithm 1. Since our cell model only predicts the voltage, the model cannot estimate the lifetime directly. To guess the expected lifetime for each use sequence, we emulate the voltage trace according to the use sequence until the cell voltage becomes lower than the cut-off voltage which is threshold of device shutdown. Here, C stands for the cell information which includes all the required information such as SoH, SoC, designed capacity, and time of consecutive discharging. We first determine the number of discharging cells (line 27). The use sequence is acquired by the *SeqGen* function (line 30). At every switching interval T, the discharging cells change according to the use sequence (line 32). The voltage of each cell is calculated via the cell model (line 35), and the expected lifetime is determined when a

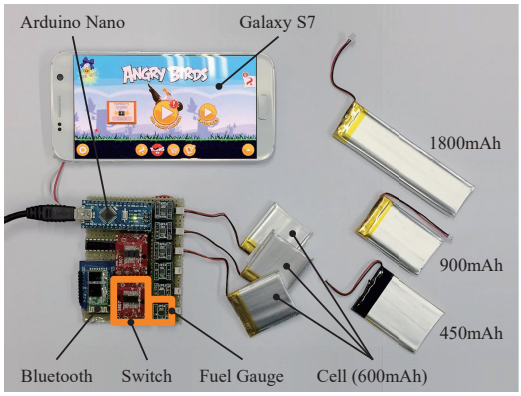

Figure 9: The prototype BattMan hardware.

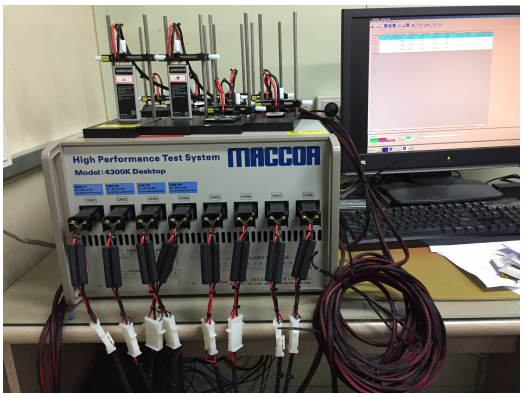

Figure 10: Experiment settings for cycling tests with Maccor 4300K.

cell voltage goes down under the cut-off voltage (line 36-37). When a cell's voltage reaches the cut-off voltage, all other cells would exhibit the similar state since all cells have been balanced. After repeating this process N times, the best use sequence is finally selected (lines 38-39).

When to perform the algorithm. Since the expected battery lifetime depends on the discharging current and the recovery time, the cell use policy should be changed accordingly. However, since an instantaneous current drain of a mobile device is highly dependent on the user's usage patterns, it is hardly possible to predict the discharging current in the future. In addition, the computation overhead of running Algorithm 1 on mobile device is not negligible. Therefore, we pre-calculate the number of discharging cells for each discharging current, SoH, and SoC, i.e., the results of Algorithm 1. We store them in a table and use it at runtime. BattMan continuously monitors average discharging current in a sliding window and simply selects the number of discharging cells from the table. This method minimizes the overhead without performance degradation.

Difference over prior art. A number of previous works tried to prolong battery lifetime using the rate capacity or the recovery effect [5, 7, 21, 27, 34]. However, none of them considered recovery effect, rate capacity effect, and SoH *concurrently*. In multi-cell battery system, exploiting the recovery effect and the rate capacity effect is necessary to maximize battery lifetime. SoH is another key factor that determines battery lifetime. Without being considered SoH, the cell with the lowest SoH would be shut down earlier than the others, significantly reducing the opportunity to use the recovery and rate capacity effects. Since the proposed WSRR scheme considers recovery effect, rate capacity effect, and SoH all at the same time, the best use policy is selected to maximize battery lifetime.

4 IMPLEMENTATION

The implementation of BattMan requires both software and hardware components. The BattMan software is composed of a mobile application and the Arduino program. The mobile application receives various information about cells, such as SoC, SoH, and discharging current information, from the BattMan hardware, then performs Algorithm 1.

We built BattMan hardware that is attached to a mobile device. Figure 9 shows the prototype hardware implementation. The BattMan hardware monitors various information required for running Algorithm 1 and sends it to the mobile application via Bluetooth. Upon receiving the usage policy from the mobile application, the hardware controls the cells according to the determined use policy. The BattMan hardware has six power supply channels. The NPN power transistors are used to connect the battery to the mobile device. We used the dual channel NPN power MOSFET to control the battery's discharging with a small form factor. The MOSFET of each channel is controlled by an on/off signal from Arduino Uno. Each channel has a fuel gauge IC (i.e., STC3100 [3]) to read the cell voltage and the current flow. The fuel gauge IC communicates with the I^2C protocol, which identifies a node using a unique address to transmit data. Since our fuel gauge ICs have the same address, the I^2C protocol cannot individually discern among them. Hence, we used MUX/DEMUX to connect one fuel gauge IC at a time.

5 EVALUATION

We validated the proposed battery cell model and subsequently evaluated the performance of BattMan in a controlled environment and as well as with real usage scenarios. First, our cell model is evaluated in terms of accuracy and effectiveness in extending battery lifetime. Second, the performance of the cell scheduling algorithm is validated with the experiments under various environments together with its overhead analysis. Finally, we analyzed the relationship between various factors such as the number of cells, degree of cell aging, cell model, cell switching interval, and sensing window for discharging current.

5.1 Experimental Setup

In order to conduct the experiments for the proposed scheme, we should construct various forms of multi-cell batteries to use with mobile devices. Specifically, we should evaluate the efficacy of BattMan by comparing the lifetime of a multi-cell battery over a single-cell one of the same overall capacity. In our present work, we constructed a battery system of 1800mAh for the experiment. In fact, most recent smartphones are equipped with around 3000mAh of battery, but we specifically targeted a 1800mAh battery due to

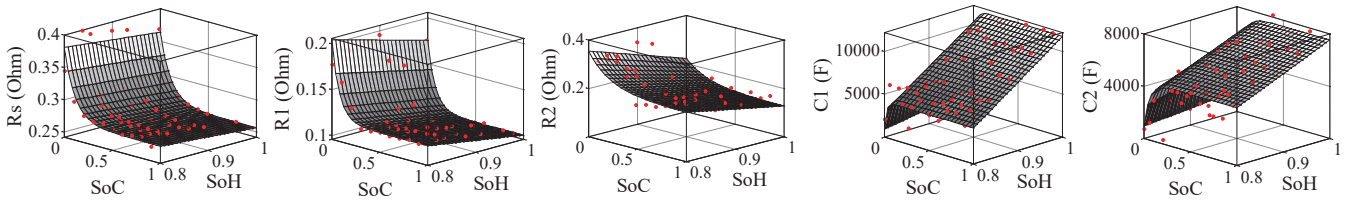

Figure 11: The RC network components for the 600mAh battery cell.

the ease of construction of multi-cell battery with the off-the-shelf battery cells. That is, in order to build various configurations of multi-cell batteries providing the same capacity, we used small cells of different capacity in a modular fashion. Among the battery cells available in the market, we selected Power Source Energy [2]'s Li-ion batteries of 450mAh, 600mAh, 900mAh, and 1800mAh to construct a four-cell, a three-cell, a two-cell, and a single-cell battery, respectively, all of which provide the same overall capacity of 1800mAh. These cells have a cut-off voltage of 3.0V, a maximum discharging rate of 1.2C, and a maximum charging rate of 0.25C. For the accurate measurement of battery cell characteristics, we used the Maccor 4300K cycler shown in Figure 10.

5.2 Model Accuracy

BattMan selects the cells to use next based on the underlying battery cell model, hence model accuracy is critical for overall performance of the system. We evaluated the accuracy of the proposed cell model in various conditions including discharging current, cell aging, and relaxation frequency. The results are compared with the ground truth measured by the Maccor cycler. First, we experimentally acquired the coefficients for the model explained in Section 3.2, that is, R_s, R_1, R_2, C_1, and C_2 values, under various conditions. In detail, we measured the cell voltage while discharging 0.4C, 0.8C, and 1.2C of current and resting one hour at every 10% of SoC. This process was repeated for seven levels of SoH from 1.0 to 0.8. The SoH level of cell was obtained with the cycler by controlling the number of charging/discharging cycles at room temperature. The experiments were conduced for each type of cell used in the expeirment: i.e., 450mAh, 600mAh, 900mAh, and 1800mAh. Figure 11 shows the experimental result for the 600mAh cell. Based on the results, the coefficient of Equation (7) for the 600mAh cell is determined as:

$$R_s = (0.220 \cdot \exp(-8.96 \cdot SoC) + 0.528) \cdot (-0.114 \cdot SoH + 0.600)$$
$$R_1 = (0.674 \cdot \exp(-12.6 \cdot SoC) + 0.904) \cdot (-0.0919 \cdot SoH + 0.203)$$
$$R_2 = (0.176 \cdot \exp(-4.46 \cdot SoC) + 0.237) \cdot (-1.61 \cdot SoH + 0.2.14)$$
$$C_1 = 1000 \cdot (-2.24 \cdot \exp(-40.0 \cdot SoC) + 2.88) \cdot (13.1 \cdot SoH - 9.02)$$
$$C_2 = 10000 \cdot (-1.79 \cdot \exp(-16.2 \cdot SoC) + 2.29) \cdot (0.68 \cdot SoH - 0.349)$$

Similarly, we acquired the coefficients for 450mAh, 900mAh, and 1800mAh cells.

We validated the accuracy of the proposed cell model in various aspects. First, we verify that our model reflects cell aging successfully. For the experiment, we used two different cells of 1800mAh and 450mAh whose SoH level was 0.9 (i.e, moderately aged). The two cells were discharged with the constant current 0.8C and 0.4C, respectively. Figure 12 shows the voltage traces of our model in comparison with both the existing circuit model and the ground truth measured with the Maccor cycler. Figure 12(a) shows that our model is closely matching to the ground truth, whereas the existing circuit model overestimates the voltage because of its inability to consider the effect on cell aging. Similarly, for the case of Figure 12(b) where the cell rests while discharging current, the existing circuit model does not predict the voltage trace accurately, whereas our model fits to the ground truth.

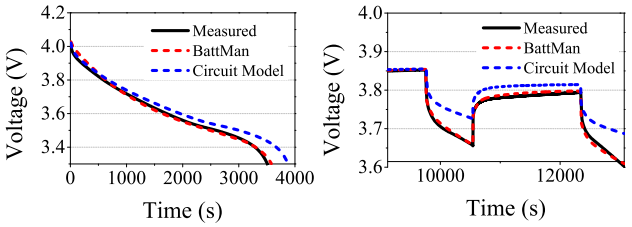

(a) 0.8C, 1800mAh cell **(b) 0.4C, 450mAh cell**

Figure 12: Model accuracy on cell aging (SoH 0.9).

Second, we evaluated the accuracy of our model estimating the capacity gain due to recovery effect. The capacity gain $C_{recovered}$ in Equation (8) is obtained by comparing the amount of used capacity when a cell is discharged *intermittently* with when a cell is discharged *continuously* by the cycler. For the experiments, we repeatedly conducted the measurements for various combination cell parameters, since the recovery effect is influenced by factors such as SoH, discharging current, and the duration of discharging and recovery (i.e., recovery interval). We then calculated the recovery coefficient ρ via a data fitting process on Equation (8). In our experiment setup, the ρ value was finally determined as 0.0738 for all cells. Based on this ρ value, the capacity gain was estimated and compared with the actual capacity gain. Figure 13 shows the estimation error of the proposed model on the recovered effect. We used a set of different discharging current for the measurement, ranging between 0.4C and 1.2C. The experiment results reveal that the overall error rate is considered acceptable, although the accuracy of our model varies due to the complicated relationship between the amount of recovered capacity and SoH.

Finally, we evaluated the overall accuracy of our model by conducting the experiments repeatedly with the combination of SoH level and the different cell capacities under various levels of discharging currents. For the ground truth measurement, we discharged a cell intermittently with a constant current and recorded the voltage of cell using the cycler. The error rate of our cell model is then calculated by comparing the estimation result with the ground truth every one second. Figure 14 shows the result. The average error rate, which is calculated over all cases of discharging current, is 1.08%, while the maximum error is 4.08%. This means that until the voltage drops under cut-off, our model predicts the voltage with an

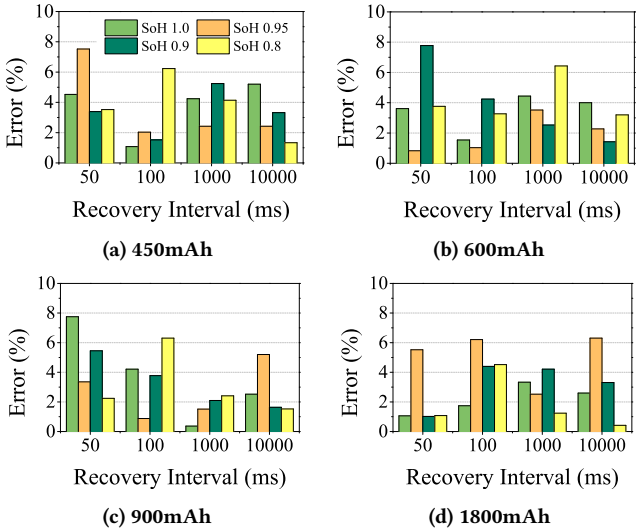

(a) 450mAh (b) 600mAh

(c) 900mAh (d) 1800mAh

Figure 13: Model accuracy on the capacity gain due to recovery effect.

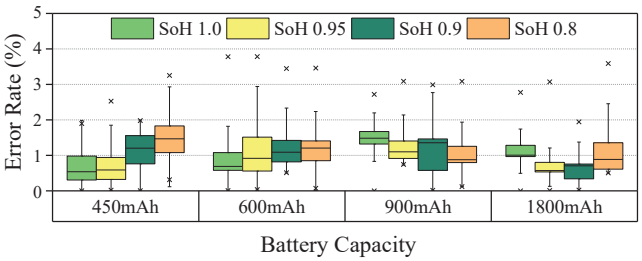

Figure 14: Model accuracy for combined cases.

average 1% error rate. The results indicate that the proposed model reflects various factors of discharging current, SoH, and recovery effect accurately.

5.3 Efficacy of Cell Scheduling

The cell scheduling algorithm of BattMan aims to select an adequate set of discharging cells to maximize the lifetime of battery. To validate the performance of the proposed algorithm, we evaluated whether BattMan selects the best use policy for cells under various conditions.

We measured the lifetime gain of BattMan under various discharging current and SoH. The overall capacity of multi-cell configuration used in the experiment is 1800mAh. The lifetime gain is calculated by comparing the lifetime of multi-cells configuration to that of a single-cell battery. To determine the cell use policy according to discharging current and to switch cells, we need to fix the sensing window for discharging current monitoring and the cell switching interval for the experiment. Considering the hardware specification and overhead, we set the sensing window and the switching interval as 200 ms and 50 ms, respectively. The effect of these factors on lifetime is analyzed in Section 5.5.

Figure 15 shows the lifetime gain of each use policy according to discharging current. The cell use policy selected by our algorithm is represented by the red arrows. For example, Figure 15(b) shows the results for the case when, we use a three-cell configuration and three different use policies are evaluated according to the number of discharging cells. Here, "1 cell" means the BattMan algorithm is discharging one cell at a time, whereas "3 cells" represents discharging three cells at a time. Figure 15(a-c) show the result for the new cells (SoH 1.0), while Figure 15(d-f) represent the results of aged cells (SoH 0.8). Figure 15(a) shows, for instance, the case of exploiting two-cell configuration. When the discharge current is higher than 1000 mA, the best use policy is to discharge the cells

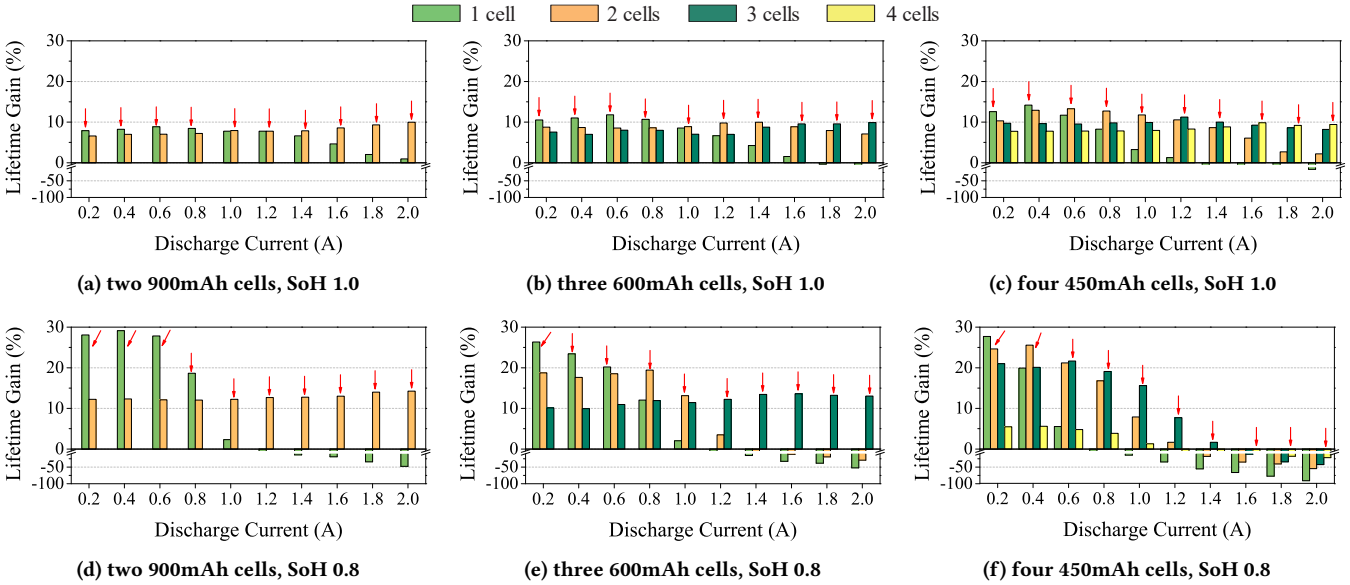

(a) two 900mAh cells, SoH 1.0 (b) three 600mAh cells, SoH 1.0 (c) four 450mAh cells, SoH 1.0

(d) two 900mAh cells, SoH 0.8 (e) three 600mAh cells, SoH 0.8 (f) four 450mAh cells, SoH 0.8

Figure 15: Lifetime gain of multi-cell configurations over single-cell system according to cell use policy.

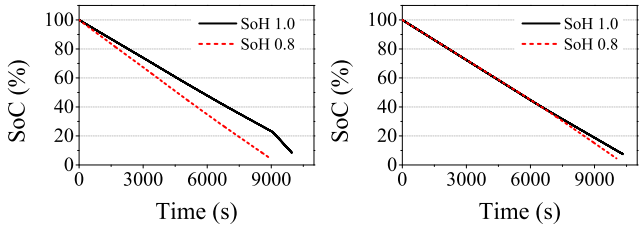

(a) Existing cell model **(b) BattMan model**

Figure 16: Effect of cell model upon cell scheduling.

concurrently, thus maximizing the gain of the rate capacity effect. Alternatively, when the discharging current is under 1000 mA, the continuous switching of the cells to maximize the recovery effect showed the maximum gain. Figure 15(c) shows the similar results with four-cell configuration. In contrast with the case of two-cell configuration, the best policy with 600~1000 mA is to discharge two cells while recovering the remaining two cells. This is because when the discharging current for an individual cell is lower than a certain level, the recovery effect is dominant over the rate capacity effect. These results indicate that BattMan always selects the best use policy to maximize the lifetime.

Figure 15(d-f) shows that the lifetime gain changes according to SoH. With SoH 1.0, the lifetime improves with the increased number of cells under 1.2A, because the larger number of cells offers more opportunities to recover and also to reduce the amount of discharging current for each cell. Therefore, the four-cell configuration generally showed the largest lifetime gain. However, in SoH 0.8, the two-cell configuration showed the largest gain. Since the internal resistance of small-capacity cell grows up faster than large-capacity cell, the amount of voltage drop for small cell is greater than large cell, leading the shortened lifetime. In fact, the lifetime of four-cell configuration was even shorter than a single-cell configuration under high discharging current. The results also indicate that BattMan accurately determines the best usage policy under a varying degree of SoH.

Meanwhile, we evaluated the impact of the battery cell model upon the performance of cell scheduling. We compared the proposed cell model with the existing circuit model in terms of overall battery lifetime. For the experiment, we used a two-cell configuration where each cell has a different SoH of 1.0 and 0.8. We repeated the experiment of the "1 cell" case in Figure 15 with 0.4A of discharge current. We also traced the SoC of cells to analyze the efficiency of each cell model. Figure 16(a) and (b) show the SoC trace of each cell for the existing circuit model and our model, respectively. The lifetime of existing cell model is 9971 seconds while 10333 seconds for the proposed cell model. The battery lifetime of the existing cell model is reduced because the voltage of each cell becomes unbalanced due to its inability to reflect SoH. On the other hand, Figure 16(b) shows that SoC of each cell for our model is well balanced, and consequently its lifetime is extended.

5.4 Real Usage Scenario

Thus far, the evaluation was conducted under a controlled environment using the battery cycler. We now evaluate the performance of BattMan with real mobile devices. For the experiment, we used two

Table 1: Applications used in real scenario. Power is measured in Galaxy S7 smartphone.

App.	Average power	Duration	Description
Youtube	2933 mW	180 s	Search videos and watch.
Temple Run 2	2658 mW	300 s	Play first stage 3 times.
Facebook	2452 mW	180 s	Refresh newsfeed and send messages.
Gmail	2110 mW	180 s	Refresh inbox and read.
Chrome	1898 mW	240 s	Create a new tap, search and read articles.
Instagram	1900 mW	180 s	Refresh newsfeed and search users.
Skype	1736 mW	180 s	Find a friend and call.
Line	1631 mW	120 s	Check new messages and reply.
Android Calculator	1569 mW	120 s	Calculate arithmetic operations.

different types of smartphones: Samsung Galaxy S7 and Samsung Galaxy Note 4. First, we collected the actual usage patterns of nine popular Android applications from a brief in-lab test and generated a Monkey script [1] to repeat the usage patterns for the experiment. Table 1 summarizes the application information used for the experiments. The length of the overall scenario is 1680 seconds, and the average discharging current is 562.8mA for Galaxy S7 and 763.4mA for Galaxy Note 4.

We compared the lifetime gain of BattMan with two simple discharging policies: i.e., (1) continuously switch cells to maximize recovery effect (RE-only), and (2) discharge all cells concurrently to maximize rate capacity effect (CE-only). For example, with four-cell configuration, RE-only uses one cell at a time and the remaining three are in the idle state, which is in fact equivalent to the leftmost bars in Figure 15. CE-only always uses four cells concurrently. This is represented as the rightmost bars in Figure 15. The experiment was conducted with the two-cell, three-cell, and four-cell configuration for both Galaxy S7 and Galaxy Note 4. The number of cells and the SoH factor are also considered for the experiments. Table 2 shows the summary of the results. In all cases, BattMan outperforms both RE-only and CE-only, extending the battery lifetime upto 13.94% for SoH 1.0 while 18.44% for SoH 0.8 for Galaxy S7. With SoH 1.0, RE-only generally showed longer lifetime than CE-only because as shown in Figure 15, RE-only outperformed CE-only under 600 mA. However, in SoH 0.8, CE-only improved lifetime more than RE-only due to the large internal resistance as described in Section 5.3. In both cases, BattMan extends lifetime the most because the scheme applies the use policy selectively. Unlike RE-only and CE-only, BattMan finds the use policy effectively according to SoH and discharging current. With SoH 1.0, BattMan selected the use policy which maximize the recovery frequency, whereas the scheme minimized discharging current for each cell with SoH 0.8. Overall, the proposed scheme is indeed practical since BattMan extends lifetime significantly without any QoS degradation.

5.5 Sensitivity Analysis

As discussed above, BattMan's performance is affected by various factors such as the number of cells, SoH, switching interval, and

Table 2: Battery lifetime comparison with real usage scenarios.

SoH = 1.0	Lifetime (sec)									
System	Single-cell	RE-only			CE-only			BattMan		
# of cells	1	2	3	4	2	3	4	2	3	4
S7	10456	11106 (+6.22%)	11148 (+6.62%)	11370 (+8.74%)	11042 (+5.60%)	11149 (+6.63%)	11085 (+6.02%)	11276 (+7.84%)	11504 (+10.02%)	**11914 (+13.94%)**
Note4	7535	8042 (+6.73%)	7766 (+3.07%)	7870 (+4.45%)	8034 (+6.62%)	7854 (+4.23%)	7959 (+5.63%)	8154 (+8.21%)	8261 (+9.64%)	**8471 (+12.42%)**

SoH = 0.8	Lifetime (sec)									
System	Single-cell	RE-only			CE-only			BattMan		
# of cells	1	2	3	4	2	3	4	2	3	4
S7	8104	9370 (+15.62%)	9078 (+12.02%)	8450 (4.27%)	9017 (+11.27%)	8959 (+10.55%)	8369 (+3.27%)	**9598 (+18.44%)**	9388 (+15.84%)	9164 (+13.08%)
Note4	5608	6329 (+12.86%)	6084 (+8.49%)	4348 (-22.47%)	6263 (+11.68%)	6196 (+10.49%)	5669 (+1.09%)	**6497 (+15.85%)**	6296 (+12.27%)	6098 (+8.74%)

the monitoring duration of discharging current. We analyzed the effect of each individual factor on the lifetime of BattMan. Again, the experiments were conducted with the real usage scenarios in Table 1 on Galaxy S7. For this experiment, we used the two-cell configuration since it delivered the largest lifetime gain in Section 5.4. Here, the lifetime again is acquired by comparing the lifetime of multi-cell configuration with the single-cell configuration.

First, we analyzed the effect of cell aging on lifetime because the degree of cell aging affects both rate capacity effect and recovery effect. Figure 17 shows the lifetime according to SoH. The internal resistance increases along with SoH, hence the lifetime itself decreases with cell aging. However, the lifetime gain increases because the amount of discharging current is large in a single-cell configuration, leading to more voltage drop.

Next, we analyzed the effect of the cell switching interval. Since BattMan extends the lifetime using recovery effect, the switching interval, which determines the recovery frequency, affects the battery lifetime. To observe the impact of the switching interval, we measured the lifetime gain depending on the length of switching interval. Figure 18 shows the result. With SoH 1.0, the lifetime gain decreases from 8% to 3%, while the gain sharply decreases from 18% to 8% with SoH 0.8, because the amount of lifegain in SoH 0.8 is larger than SoH 1.0. Nevertheless, the overall trend is similar in both cases. The lifetime gain decreases according to switching interval because the lengthened switching interval decreases the frequency of recovery. The experiment indicates that the switching interval should be minimized to prolong the lifetime.

We also evaluated the effect of the sensing window for monitoring the discharging current. Figure 19 shows the lifetime according to the sensing window. Over a certain length of window, the lifetime decreases because the system does not select the use policy accurately due to the inaccuracy in monitoring discharging current. In particular, when SoH is low, the increased internal resistance causes voltage drop significantly. Therefore, missing the occurrence of high discharge current is critical for cells in low SoH. The difference under one second is not significant, however. We consider that sensing the discharging current every one second is unlikely to cause heavy workload in chip-level, hence one second of sensing window would guarantee the lifetime gain.

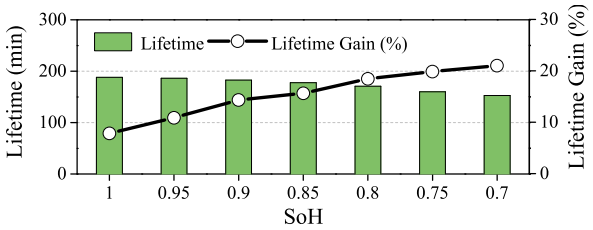

Figure 17: Battery lifetime according to SoH.

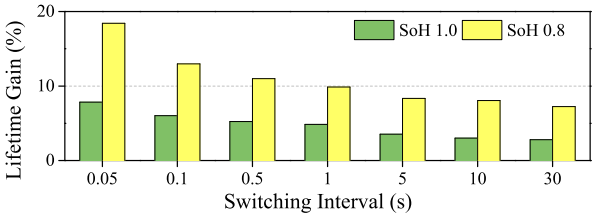

Figure 18: Effect of switching interval.

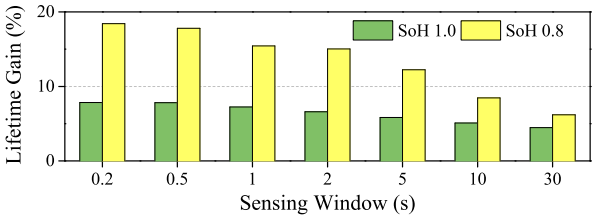

Figure 19: Effect of sensing window for current monitoring.

5.6 Overhead

The runtime overhead of BattMan is critical, because BattMan should continuously determine an adequate set of discharging cells. With non-negligible overhead, the overall system will degrade user experience. We observed the overhead incurred by the repeated calculations in the BattMan application. The CPU overhead was observed under 0.5%. This indicates that BattMan does not affect the overall performance of mobile devices.

6 DISCUSSION

In the present work, we validated the proposed system using the Galaxy S7 and Galaxy Note 4. Since the aging process, recovery

effect and rate capacity effect are common characteristics of the Li-ion battery, we believe that our system will also extend the lifetime for other types of mobile devices that use Li-ion batteries. In addition, the proposed model will be fitted to a new device model after a brief learning phase. Since the learning phase can be easily done by the manufacturer in the production process, we consider our work to be practical.

Temperature is one of the factors that could cause errors in our model, because the discharging profile is affected by temperature [19]. Also, internal resistance, which increases as the temperature goes high, influences the accuracy of our models. Therefore, we controlled the environment by ensuring it was as stable as possible and evaluated the scheme only with new batteries to avoid external influences due to product deviation. Temperature issues will further be considered in our subsequent study.

Considering the practical use of the proposed system for mobile devices, we should consider the optimal number of cells for multi-cell battery system. We observed that the optimal number of cell changes according to SoH in an interesting way. Under high SoH, lifetime increases with the increased number of cells, whereas two-cell configuration is adequate in low SoH. From the pragmatic viewpoint, however, a small number of cells for battery would be preferred because we could reduce the hardware costs and the systems overhead that are required for monitoring and switching batteries. Therefore, we would suggest that the reasonable number of cells for the use of recent smartphones is practically two, considering both efficiency and effectiveness of the scheme. Note that in the present work, we did not consider the cost issue, because the main purpose of the present work is to validate the possibility of a multi-cell battery system for mobile devices.

7 RELATED WORK

7.1 Battery Modeling

Extensive attempts have been made to model battery characteristics. The circuit models regard a battery as a composition of circuit components. Each of model has an unique configuration of circuit components. They varies from the most simple model with only resistor [28] to the most complex model with three RC networks [18], but the runtime base two RC network model [10] which is used by BattMan cell model is commonly used. [32] developed an impedance-based model considering aging effect by exploiting the AC response characteristics of the battery. This model is, however, requires unique equipment to measure internal impedance of battery at wide range of frequency, resulting high cost for modeling. The physics-based models are presented based on the dynamics of Li-ion batteries in [26]. Doyle et. al [14] and Thomas [31] proposed a model to reflect the electrochemical characteristics of the battery. Rakhmatov and Vrudhula [29, 30] proposed a model focusing on diffusion in battery material. However, the model complexity is not acceptable in the mobile environment, because a large number of parameters are required and the equations are too complex. KiBaM [24] proposed an intuitive model and tried battery modeling based on their chemical kinetic processes. Both the rate capacity and recovery effects are considered in their model, but the target battery is Lead-acid, which is not applicable to mobile devices. Focusing on the recovery effect, prior work has shown that battery life can indeed be extended. [4, 12] developed a stochastic model using a Markov chain, and applications are proposed. They considered a probability to recover, not the exact voltage recovery process.

7.2 Multi-cell Battery System

The multi-cell battery system is widely studied in the EV field. [6] tried to apply the recovery effect to an EV application, but only a limited scenario was considered. The recent work of [9] used the recovery effect in sensor networks to extend lifetime. Especially, [34] designed a recovery effect model for mobile devices and extended battery lifetime for the case of video streaming. However, neither switching algorithm is presented nor the description on its hardware implementation. Recently, [5] designed a multi-cell battery system considering API for the operating system to control the battery. However, they only proposed the concepts and did not report the result of real usage scenario test.

Under multi-cell battery environments, battery lifetime can be extended via well-designed cell scheduling. One intuitive scheduling method is round robin [8], which simply switches cells continuously. [7] tried to select discharging cells dynamically according to discharging current, but the scheme simply switches every cell very fast to split load. Previous work of this field [21] established unique battery models along with the scheduling algorithm for EV application, but the cell aging (i.e., SoH) effect is not considered. Studies on reconfigurable battery pack [13], which allow to change the cell connections in real time have possibility to extend battery lifetime but hardly applicable, due to the insufficient consideration of the battery model and cost of hardware implementation.

8 CONCLUSION

In this paper, we proposed BattMan, a multi-cell battery system for mobile devices to increase battery lifetime. To the best of our knowledge, BattMan is the first approach to model the battery cell in mobile devices considering the factors such as rate capacity effect, recovery effect, and cell aging. The cell scheduling is another contribution of our work. The scheme maximizes battery lifetime on different current draws, based on the combined use of rate capacity and recovery effect.

We believe that the multi-cell battery system would provide a new opportunity for solving battery issues even in mobile devices. Together with many software-based methods, the proposed scheme will be able to generate synergistic effects on battery lifetime. We plan to extend our research by combining the scheme with diverse kinds of software-based techniques.

ACKNOWLEDGMENTS

This work was supported by Samsung Research Funding Center of Samsung Electronics under project number SRFC-TB1503-02.

REFERENCES

[1] 2017. Android Monkey script. (2017). http://developer.android.com/tools/help/monkey.html
[2] 2017. Power Source Energy. (2017). http://www.psebattery.com/en_US/index.asp
[3] 2017. STMicroelectronics, STC3100. (2017). http://www.st.com/en/power-management/stc3100.html
[4] Maria Adamou and Saikat Sarkar. 2003. A framework for optimal battery management for wireless nodes. *IEEE Journal on Selected Areas in Communications* 21, 2 (2003), 179–188.

[5] Anirudh Badam, Ranveer Chandra, Jon Dutra, Anthony Ferrese, Steve Hodges, Pan Hu, Julia Meinershagen, Thomas Moscibroda, Bodhi Priyantha, , and Evangelia Skiani. 2015. Software Defined Batteries. In *Proceedings of the 25th Symposium on Operating Systems Principles (SOSP)*. ACM, Monterey, CA, USA, 215–229.

[6] Andreas Baumgardt, Florian Bachheibl, and Dieter Gerling. 2014. Utilization of the battery recovery effect in hybrid and electric vehicle applications. In *17th International Conference on Electrical Machines and Systems (ICEMS)*. IEEE, Hangzhou, China, 254–260.

[7] Luca Benini, D. Bruni, Maria A. Mach, Enrico Macii, and Massimo Poncino. 2003. Discharge current steering for battery lifetime optimization. *IEEE Trans. Comput.* 52, 8 (2003), 985–995.

[8] Luca Benini, Gabriella Castelli, Alberto Macii, Enrico Macii, Massimo Poncino, and R. Scarsi. 2001. Extending Lifetime of Portable Systems by Battery Scheduling. In *Proceedings of the Conference on Design, Automation and Test in Europe (DATE)*. IEEE, Piscataway, NJ, USA, 197–203.

[9] Chi-Kin Chau, Fei Qin, Samir Sayed, Muhammad H. Wahab, and Yang Yang. 2010. Harnessing battery recovery effect in wireless sensor networks: Experiments and analysis. *IEEE Journal on Selected Areas in Communications* 28, 7 (2010), 1222–1232.

[10] Min Chen and Gabriel A. Rincon-Mora. 2006. Accurate electrical battery model capable of predicting runtime and I-V performance. *IEEE Transactions on Energy Conversion* 21, 2 (2006), 504–511.

[11] Xiaomeng Chen, Abhilash Jindal, Ning Ding, Yu Charlie Hu, Maruti Gupta, and Rath Vannithamby. 2015. Smartphone Background Activities in the Wild: Origin, Energy Drain, and Optimization. In *Proceedings of the 21st Annual International Conference on Mobile Computing and Networking (MobiCom)*. ACM, New York, NY, USA, 40–52.

[12] Carla F. Chiasserini and Ramesh R. Rao. 1999. Pulsed Battery Discharge in Communication Devices. In *Proceddings of the 5th Annual ACM/IEEE International Conference on Mobile Computing and Networking (MobiCom)*. ACM, Seattle, WA, USA, 88–95.

[13] Song Ci, Jiucai Zhang, Hamid Sharif, and Mahmoud Alahmad. 2007. A novel design of adaptive reconfigurable multicell battery for power-aware embedded networked sensing systems. In *IEEE Global Telecommunications Conference (GLOBECOM)*. IEEE, Washington, DC, USA, 1043–1047.

[14] Marc Doyle, Thomas F. Fuller, and John Newman. 1993. Modeling of galvanostatic charge and discharge of the lithium/polymer/insertion cell. *Journal of the Electrochemical Society* 140, 6 (1993), 1526–1533.

[15] Liang He, Lipeng Gu, Linghe Kong, Yu Gu, Cong Liu, and Tian He. 2013. Exploring adaptive reconfiguration to optimize energy efficiency in large-scale battery systems. In *the 34th Real-Time Systems Symposium (RTSS)*. IEEE, Vancouver, Canada, 118–127.

[16] Xiaosong Hu, Shengbo Li, and Huei Peng. 2012. A comparative study of equivalent circuit models for Li-ion batteries. *Journal of Power Sources* 198, 15 (2012), 359–367.

[17] Yiran Hu and Steve Yurkovich. 2011. Linear parameter varying battery model identification using subspace methods. *Journal of Power Sources* 196, 6 (2011), 2913–2923.

[18] Yiran Hu, Steve Yurkovich, Yann Guezennec, and B. J. Yurkovich. 2011. Electro-thermal battery model identification for automotive applications. *Journal of Power Sources* 196, 1 (2011), 449–457.

[19] Ala A. Hussein. 2015. Experimental modeling and analysis of lithium-ion battery temperature dependence. In *IEEE Applied Power Electronics Conference and Exposition (APEC)*. IEEE, Charlotte, NC, USA, 1084–1088.

[20] Shugang Jiang. 2011. *A parameter identification method for a battery equivalent circuit model*. SAE Technical Paper.

[21] Hahnsang Kim and Kang G. Shin. 2009. Scheduling of Battery Charge, Discharge, and Rest. In *the 30th Real-Time Systems Symposium (RTSS)*. IEEE, Washington, DC, USA, 13–22.

[22] Michael Knauff, Jeffrey McLaughlin, Chris Dafis, Dagmar Niebur, Pritpal Singh, Harry Kwatny, and Chika Nwankpa. 2007. Simulink model of a Lithium-ion battery for the hybrid power system testbed. In *Proceedings of 2007 the ASNE Intelligent Ships Symposium*. IEEE, 1–8.

[23] Seongjun Lee, Jonghoon Kim, Jaemoon Lee, and Bo H. Cho. 2008. State-of-charge and capacity estimation of lithium-ion battery using a new open-circuit voltage versus state-of-charge. *Journal of Power Sources* 185, 2 (2008), 1367–1373.

[24] James F. Manwell and Jon G. McGowan. 1993. Lead acid battery storage model for hybrid energy systems. *Solar Energy* 50, 5 (1993), 399–405.

[25] Marcelo Martins, Justin Cappos, and Rodrigo Fonseca. 2015. Selectively Taming Background Android Apps to Improve Battery Lifetime. In *Proceedings of USENIX Annual Technical Conference (USENIX ATC)*. USENIX Association, Santa Clara, CA, USA, 563–575.

[26] John Newman and William Tiedemann. 1975. Porous-electrode theory with battery applications. *AIChE Journal* 21, 1 (1975), 25–41.

[27] Kumar Padmanabh and Rajarshi Roy. 2006. Maximum lifetime routing in wireless sensor network by minimizing rate capacity effect. In *International Conference on Parallel Processing Workshops (ICPPW)*. IEEE, Columbus, OH, USA, 167–174.

[28] Gregory L. Plett. 2004. Extended Kalman filtering for battery management systems of LiPB-based HEV battery packs Part 1. Background. *Journal of Power Sources* 134, 2 (2004), 252–261.

[29] Daler Rakhmatov. 2009. Battery Voltage Modeling for Portable Systems. *ACM Transactions on Design Automation of Electronic Systems (TODAES)* 14, 2 (2009), 21–36.

[30] Daler Rakhmatov and Sarma Vrudhula. 2001. An Analytical High-level Battery Model for Use in Energy Management of Portable Electronic Systems. In *Proceedings of the 2001 IEEE/ACM International Conference on Computer-aided Design (ICCAD)*. IEEE, Piscataway, NJ, USA, 488–493.

[31] Karen E. Thomas, Robert M. Darling, and John Newman. 2002. *Advances in lithium-ion batteries: Mathematical modeling of lithium batteries*. New York: Springer-Verlag.

[32] Uwe Troltzsch, Olfa Kanoun, and Hans-Rolf Trankler. 2011. Characterizing aging effects of lithium ion batteries by impedance spectroscopys. *Electrochimica Acta* 51, 8–9 (2011), 1664–1672.

[33] Po-Hsien Tseng, Pi-Cheng Hsiu, Chin-Chiang Pan, and Tei-Wei Kuo. 2014. User-Centric Energy-Efficient Scheduling on Multi-Core Mobile Devices. In *Proceedings of the 51st ACM/IEEE Design Automation Conference (DAC)*. IEEE, San Francisco, CA, USA, 1–6.

[34] Kun Wei, Wuxiong Zhang, and Yang Yang. 2013. Prolonging battery usage time in smart phones. In *IEEE International Conference on Communications (ICC)*. IEEE, Budapest, Hungary, 2360–2364.

[35] Xiaoqiang Zhang, Weiping Zhang, and Geyang Lei. 2016. A review of Li-ion battery equivalent circuit models. *Transactions on 2016 Electrical and Electronic Materials* 17, 6 (2016), 311–316.